GEOPHYSICAL RESEARCH LETTERS, VOL. 27, NO. 4, PAGES 505-508, FEBRUARY 15, 2000

The long-term variation of the Sun's open magnetic flux

Y.-M. Wang, J. Lean, and N. R. Sheeley, Jr.

E. O. Hulburt Center for Space Research, Naval Research Laboratory, Washington, DC

Abstract. The interplanetary magnetic field (IMF) has its origin in open magnetic regions of the Sun (coronal holes). The location of these regions and their total open flux $\Phi_{\rm open}$ can be inferred from current-free extrapolations of the observed photospheric field. We derive the long-term variation of $\Phi_{\rm open}$ during 1971–1998 and discuss its causes. Near sunspot minimum, the open flux originates mainly from the large polar coronal holes, whereas at sunspot maximum it is rooted in small, lower-latitude holes characterized by very high field strengths; the total amount of open flux thus remains roughly constant between sunspot minimum and maximum. Through most of the cycle, the variation of $\Phi_{\rm open}$ closely follows that of the Sun's total dipole strength, showing much less dependence on the total photospheric flux or the sunspot number. However, episodic increases in large-scale sunspot activity lead to strengthenings of the equatorial dipole component, and hence to enhancements in $\Phi_{\rm open}$ and the IMF strength lasting typically ~1 yr.

1. Introduction

It is now recognized that the interplanetary magnetic field strength varies over the solar cycle (see, e.g., *Slavin et al.,* 1986) and that these variations may have important terrestrial effects. Figure 1 illustrates the long-term behavior of $|B_x|$, the radial IMF strength measured near Earth, plotted as 3-month running averages from January 1971 to December 1998. Also shown are the geomagnetic *aa* index, the (inverted) Climax neutron-monitor counting rate, and the total solar irradiance based on the empirical model of *Lean et al.* [1995]. As pointed out by *Lockwood and Stamper* [1999] and E. W. Cliver (private communication, 1999), the long-term variations of $|B_x|$ and the *aa* index are remarkably similar; their correlation coefficient during 1971–1998 is 0.71, as compared with 0.28 for the correlation between *aa* index and sunspot number. As may also be seen from Figure 1 and as noted earlier by *Cane et al.* [1999], enhancements in $|B_x|$ often coincide with decreases in the cosmic ray flux (the two curves have an overall correlation of 0.72). Finally, Figure 1 shows a tendency for $|B_x|$ and the irradiance I to vary together during solar cycle 22 (see *Lockwood and Stamper,* 1999); however, this tendency is less pronounced before 1985, and the correlation coefficient over the entire 28-yr period is 0.47 (we will return to this point at the end of the paper).

Our objective here is to understand the nature and causes of the long-term variations in the IMF strength. The IMF has its source in magnetically open regions of the Sun, observed as coronal holes. *Ulysses* magnetometer measurements during 1992–1995 have demonstrated that the magnitude of the radial IMF component B_r is essentially independent of heliographic latitude and longitude at heliocentric distances $r \gg R_S$ [*Balogh et al.*, 1995]. It follows that $|B_r| \sim \Phi_{\rm open}/4\pi r^2$, where $\Phi_{\rm open}$ is the total amount of open flux (both inward and outward) threading the solar surface [*Wang and Sheeley*, 1995]. By means of a current-free extrapolation of the observed photospheric field, the global distribution of open magnetic regions may be determined and their total flux estimated for any 27.3-day Carrington rotation. We use this approach to relate the long-term variation of $\Phi_{\rm open}$ (and thus the IMF strength) to the evolution of the photospheric field.

Paper number 1999GL010744.
0094-8276/00/1999GL010744$05.00

2. Deriving the Open Magnetic Flux

We extrapolate the observed photospheric field into the corona using the source surface procedure of *Schatten et al.* [1969]. In this model, the coronal field $\mathbf{B}(r,\lambda,\phi)$ (where λ and ϕ denote respectively heliographic latitude and longitude) satisfies $\nabla\times\mathbf{B}=0$ out to a spherical "source surface" at $r = R_{ss} = 2.5\ R_S$, where the effect of the quasiradial solar-wind outflow is simulated by setting $B_\lambda = B_\phi = 0$. At the lower boundary $r = R_S$, B_r is matched to the photospheric field, which is assumed to be radially oriented [*Wang and Sheeley*, 1992]. By definition, all field lines that extend from $r = R_S$ to $r = R_{ss}$ are "open." As may be seen from Figure 2 in *Wang et al.* [1996], the open field regions derived using the model reproduce the global configuration of He I 10830 Å coronal holes throughout the solar cycle.

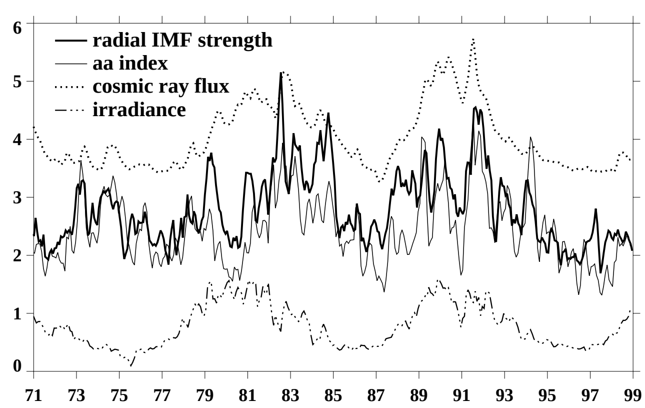

Figure 1. Long-term variation of the near-Earth radial IMF strength $|B_x|$ (nT), *aa* index (×0.1), Climax neutron-monitor counting rate (inverted), and empirically modeled total solar irradiance ($I - 1365.3$ W m^{-2}). The IMF measurements are from the NSSDC OMNIWeb data base. Here and in Figs. 2–5, all curves represent (monthly computed) 3-month running means.

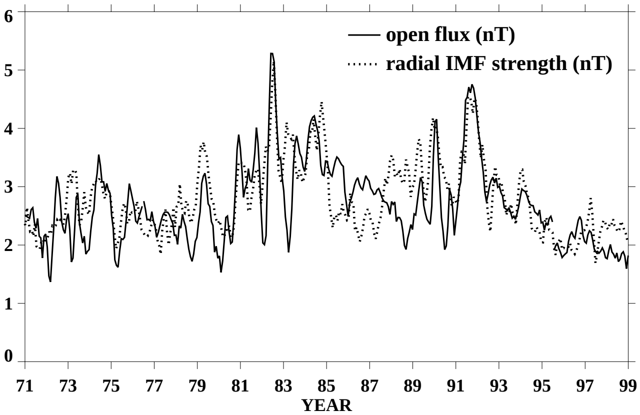

Figure 2. Variation of the Sun's total open magnetic flux $\Phi_{\rm open}$ (divided by $4\pi r_E^2$ to convert it into a field strength at 1 AU), shown together with the measured near-Earth $|B_x|$ (nT).

For the photospheric field measurements, we employ Carrington synoptic maps from the Mount Wilson Observatory (MWO) for the periods 1971–1976 and 1995–1998 and from the Wilcox Solar Observatory (WSO) for the period 1976–1995. As in *Wang and Sheeley* [1995], we correct for the saturation of the Fe I 5250 Å line profile by multiplying the measured magnetic fluxes by the latitude-dependent factor $(4.5 - 2.5 \sin^2 \lambda)$.

Figure 2 displays the calculated long-term variation of $B_{\rm open}^E \equiv \Phi_{\rm open}/(4\pi r_E^2)$, which represents the radial field strength at $r = r_E = 1$ AU on the assumption that the total open flux becomes uniformly distributed in solid angle far from the Sun. (The implied redistribution of flux beyond $r \sim 2.5$ R_S requires the presence of a current sheet and is thus not described by the source surface model.) Through most of the interval 1971–1998, $B_{\rm open}^E$ shows reasonable agreement with the measured radial IMF strength $|B_x|$ (dotted lines), both in its average magnitude and its fluctuations (the overall correlation is 0.68). Especially noteworthy is the coincidence between the large peaks in $B_{\rm open}^E$ and $|B_x|$ in 1982 and 1991. On the other hand, substantial discrepancies between the model and the observations occur during 1985–1988 and 1997–1998. A possible source of the disagreement might be the difficulty in measuring the Sun's polar fields, which reach their greatest strength near solar minimum.

3. Relation Between Open Flux and Sunspot Activity

Figure 3 compares the derived values of $\Phi_{\rm open}$ with the total photospheric flux $\Phi_{\rm tot}$, which is obtained by integrating $|B_r(R_S, \lambda, \phi)|$ over the solar surface and includes both closed and open fields; also plotted are the monthly mean sunspot numbers R_Z. It is evident that $\Phi_{\rm open}$ undergoes considerably less solar cycle modulation than does $\Phi_{\rm tot}$ or R_Z (the factors by which their respective amplitudes vary are $\sim$2, $\sim$4, and $\sim$16). The ratio $\Phi_{\rm tot}/\Phi_{\rm open}$ increases from $\sim$2–3 at sunspot minimum to $\sim$10 at sunspot maximum, when the photospheric field is dominated by closed flux in the form of active region loops. While fluctuations in $\Phi_{\rm tot}$ and R_Z are generally accompanied by fluctuations in $\Phi_{\rm open}$ (as is apparent, for example, during 1972–1975), there seems to be no simple relationship between the heights of the corresponding peaks. Moreover, in its overall envelope, the solar cycle modulation of $\Phi_{\rm open}$ (like that of $|B_x|$) lags $\Phi_{\rm tot}$ and R_Z by 1–2 yr, with its maxima occurring in 1982 and 1991, just as sunspot activity was beginning to decline. Computed for the entire interval 1971–1998, the correlation coefficient of $\Phi_{\rm open}$ and $\Phi_{\rm tot}$ is only 0.33.

One explanation for the relative constancy of $\Phi_{\rm open}$ over the solar cycle is suggested by Figure 4, which shows the variation of $A_{\rm open}$ and $\langle B_{\rm open}\rangle$, where $A_{\rm open}$ is the total surface area occupied by open flux and $\langle B_{\rm open}\rangle \equiv \Phi_{\rm open}/A_{\rm open}$ is the average field strength within these regions. It is seen that the percentage of the Sun's surface covered by open flux decreases from $\sim$20% at sunspot minimum to $\sim$5% at sunspot maximum, but that $\langle B_{\rm open}\rangle$ increases from $\sim$5 G to $\sim$20 G at the same time; thus the product $\langle B_{\rm open}\rangle A_{\rm open} = \Phi_{\rm open}$ remains roughly unchanged (cf. *Harvey et al.,* 1982). The remaining two curves in Figure 4 show that the open flux near sunspot minimum (maximum) originates mainly from latitudes above (below) 45°. These high- and low-latitude sources may be identified respectively with the large polar coronal holes present at sunspot minimum and with the smaller holes that form near active regions at sunspot maximum (see Fig. 2 in *Wang et al.,* 1996).

Further insight into the variation of the open flux may be obtained from multipole analysis. In general, the current-free coronal field may be expressed as a superposition of spherical harmonics $Y_{lm}(\lambda, \phi)$: $B_r(r, \lambda, \phi) = \sum_{l=1}^{\infty} \sum_{m=-l}^{m=l} c_l(r) a_{lm} Y_{lm}(\lambda, \phi)$, where $c_l(R_S) = 1$ and $c_l(r) \propto (r/R_S)^{-l-2}$ (see *Wang and Sheeley,* 1992). Because of the rapid decline of $(R_{ss}/R_S)^{-l-2}$ with l, only the lowest-order multipoles contribute significantly to the source surface field $B_{ss} \equiv B_r(R_{ss}, \lambda, \phi)$, and hence to $\Phi_{\rm open} = R_{ss}^2 \int |B_{ss}| d\Omega$ (where the integral is over all solid angles Ω). To measure the average strength of a given multipole l and spherical harmonic component (l, m) at the source surface, let $B_{ss} = \sum_{l=1}^{\infty} b_l(\lambda, \phi) = \sum_{l=1}^{\infty} \sum_{m=0}^{m=l} b_{lm}(\lambda, \phi)$ and define $\langle b_l\rangle \equiv \int |b_l| d\Omega/4\pi$, $\langle b_{lm}\rangle \equiv \int |b_{lm}| d\Omega/4\pi$.

Figure 5a compares the long-term behavior of $\langle b_1\rangle$, $\langle b_2\rangle$, and $\Phi_{\rm open}$. Through most of the interval 1971–1998, $\Phi_{\rm open}$ closely tracks the dipole strength $\langle b_1\rangle$ (with a correlation of 0.90); the quadrupole component $\langle b_2\rangle$ contributes signif-

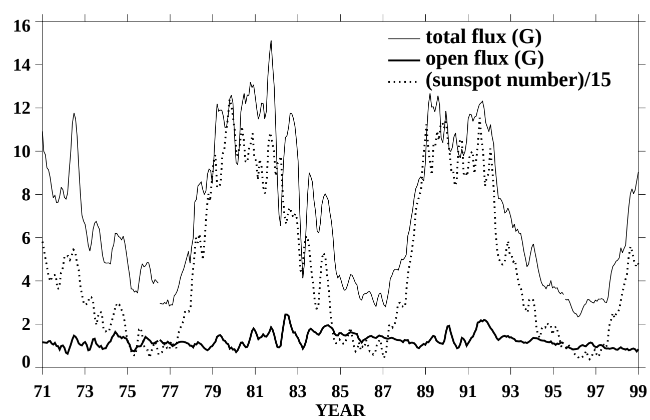

Figure 3. Variation of the total (closed and open) solar magnetic flux $\Phi_{\rm tot}$, open flux $\Phi_{\rm open}$, and sunspot number R_Z. Both $\Phi_{\rm tot}$ and $\Phi_{\rm open}$ have been divided by $4\pi R_S^2$ to convert them into equivalent field strengths (G) averaged over the solar surface.

icantly to $\Phi_{\rm open}$ only near sunspot maximum. Figure 5b shows the relation between $\Phi_{\rm open}$ and the nonaxisymmetric (equatorial) dipole strength $\langle b_{11}\rangle$; also plotted is the dipole tilt angle $\delta = \arcsin(\langle b_{11}\rangle/\langle b_1\rangle)$. It is apparent that the fluctuations in $\Phi_{\rm open}$ on timescales of $\sim$1 yr correspond to large enhancements in $\langle b_{11}\rangle$. The equatorial dipole field has its main source in the sunspot latitudes, as a comparison between the variation of $\langle b_{11}\rangle$ and that of the low-latitude open flux (Fig. 4) suggests.

The oscillatory behavior of $\langle b_{11}\rangle$ reflects the spatially and temporally nonuniform nature of sunspot activity, in which flux emerges in large active-region complexes that grow and decay on timescales of several months to more than a year (see *Gaizauskas et al.,* 1983). Since it is determined by integrating $(B_r \cos\lambda \cos\phi)$ and $(B_r \cos\lambda \sin\phi)$ over the solar surface, the strength of the equatorial dipole depends not just on the total flux within the activity complex(es), but also on the net (large-scale) longitudinal separation between the two polarities—hence the lack of a simple correlation between the heights of the peaks in $\Phi_{\rm open}$ and $\Phi_{\rm tot}$ (Fig. 3).

In Figure 6, we present butterfly diagrams (latitude-time plots) of open flux ($|B_{\rm open}|\cos\lambda$), total flux ($|B_r|\cos\lambda$), and net flux ($B_r \cos\lambda$). All of the fluxes are binned in uniform latitude intervals at the solar surface and averaged over longitude. It is seen that the low-latitude open flux tends to be "clumpy," with the larger clumps often confined to only one hemisphere and showing faint poleward extensions directed forward in time. The largest such clump occurs in 1991 in the southern hemisphere, where there is also a strong enhancement in the total flux. Comparison between the maps of open flux and net photospheric flux shows that the faint wings emanating from the clumps correspond to trailing-polarity flux surging from the sunspot latitudes toward the poles (see *Wang et al.,* 1989). It is also evident that the disappearance of the high-latitude open flux during 1971, 1979–1980, and 1989–1990 coincides with the times of polar field reversal, whereas the disappearance of the low-latitude open flux around sunspot minimum reflects the decrease in the rate of flux emergence and the migration of the net flux to the polar regions.

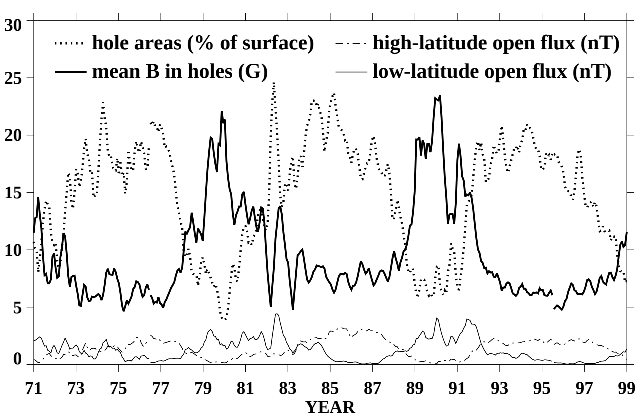

Figure 4. Variation of the total area occupied by coronal holes $A_{\rm open}/(4\pi R_S^2)$ (%), the average field strength in holes $\langle B_{\rm open}\rangle \equiv \Phi_{\rm open}/A_{\rm open}$ (G), the open flux originating from high latitudes $\Phi_{\rm open}(|\lambda| > 45°)/(4\pi r_E^2)$ (nT), and the open flux originating from low latitudes $\Phi_{\rm open}(|\lambda| < 45°)/(4\pi r_E^2)$ (nT).

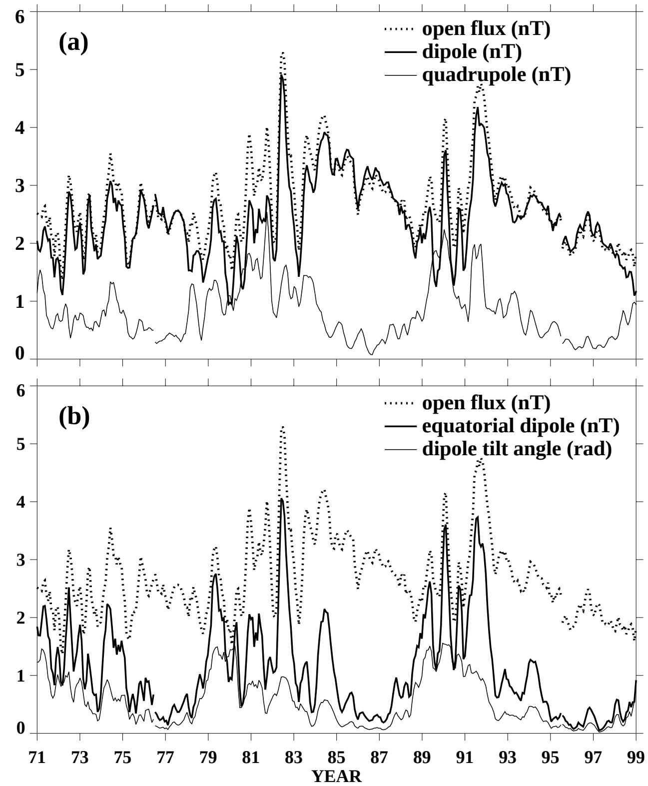

Figure 5. (a) Variation of $\langle b_1\rangle(R_{ss}/r_E)^2$, $\langle b_2\rangle(R_{ss}/r_E)^2$, and $\Phi_{\rm open}/(4\pi r_E^2)$ (all in nT). (b) Variation of $\langle b_{11}\rangle(R_{ss}/r_E)^2$ and $\Phi_{\rm open}/(4\pi r_E^2)$ (nT); also plotted is the dipole tilt angle δ, measured in radians relative to the nearest pole.

4. Conclusions

Our conclusions may be summarized as follows:

1. The variation of the radial IMF strength is similar to that of the Sun's total open flux $\Phi_{\rm open}$, as derived from source surface extrapolations of photospheric field measurements. The magnitude of the near-Earth $|B_x|$ agrees with that obtained on the assumption that $\Phi_{\rm open}$ becomes uniformly distributed in solid angle far from the Sun.

2. The variation of $\Phi_{\rm open}$ approximately follows that of the Sun's total dipole strength, except for a contribution from the magnetic quadrupole ($l = 2$) around sunspot maximum.

3. Both $\Phi_{\rm open}$ and the IMF strength show characteristic fluctuations on timescales of $\sim$1 yr, which correspond to enhancements and subsequent decay of the Sun's nonaxisymmetric dipole component. The enhancements in the equatorial dipole strength are in turn a consequence of the episodic, spatially nonuniform nature of large-scale sunspot activity (which is often distributed asymmetrically between the northern and southern hemispheres).

4. The open flux shows much less solar cycle modulation than the sunspot number or the total photospheric flux $\Phi_{\rm tot}$, which includes closed fields and is dominated by higher-order multipoles. The ratio of closed to open photospheric flux varies from $\sim$1–2 at sunspot minimum to $\sim$10 at sunspot maximum.

5. Near sunspot minimum, the open flux originates mainly from the large polar coronal holes; at sunspot maximum, it is rooted in small, strong-field regions in the activity

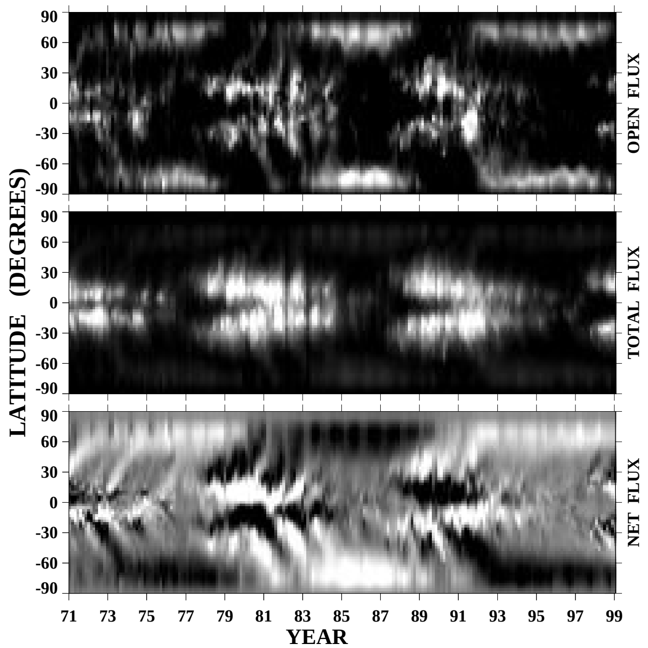

Figure 6. Latitude-time distribution of (from top to bottom) open, total, and net photospheric flux. In the upper two panels, white (black) indicates very strong (very weak) flux; in the bottom panel, white (black) indicates strong positive-polarity (strong negative-polarity) flux. The annual modulation seen in the high-latitude fluxes is an artifact caused by the Sun's 7°.25 axial tilt.

zones. The decrease in the total area occupied by coronal holes is offset by the increase in their average field strengths, with the result that $\Phi_{\rm open}$ remains roughly constant between sunspot minimum and maximum.

Our main point is that the Sun's open flux and the IMF strength are determined by the lowest-order multipoles of the photospheric field (principally the dipole component), whose variation in general does not follow that of the total photospheric flux. Returning to Figure 1, we can now understand why the total solar irradiance shows a relatively poor long-term correlation with the radial IMF strength: since its modulation reflects the competition between dark sunspots and bright plage areas [*Lean et al.*, 1995], which are both associated with closed field regions, I is a function mainly of $\Phi_{\rm tot}$, not of $\Phi_{\rm open}$ (to which I is at best indirectly related). The use of $\Phi_{\rm open}$ as an irradiance proxy [*Lockwood and Stamper*, 1999] thus seems questionable to us, unless the evolution of open and closed photospheric flux can be related quantitatively.

In a subsequent paper, we will use flux transport simulations to explore the physical relationship of open and closed fields to the emergence and decay of active regions.

Acknowledgments. We are indebted to J. T. Hoeksema (WSO/Stanford) and R. K. Ulrich (MWO/UCLA) for the magnetograph data. This work was supported by NASA and by ONR under the Solar Magnetism and Earth's Environment Research Option.

References

Balogh, A., et al., The heliospheric magnetic field over the south polar region of the Sun, *Science, 268,* 1007–1010, 1995.

Cane, H. V., G. Wibberenz, I. G. Richardson, and T. T. von Rosenvinge, Cosmic ray modulation and the solar magnetic field, *Geophys. Res. Lett., 26,* 565–568, 1999.

Gaizauskas, V., K. L. Harvey, J. W. Harvey, and C. Zwaan, Large-scale patterns formed by solar active regions during the ascending phase of cycle 21, *Astrophys. J., 265,* 1056–1065, 1983.

Harvey, K. L., N. R. Sheeley, Jr., and J. W. Harvey, Magnetic measurements of coronal holes during 1975–1980, *Sol. Phys., 79,* 149–160, 1982.

Lean, J., J. Beer, and R. Bradley, Reconstruction of solar irradiance since 1610: Implications for climate change, *Geophys. Res. Lett., 22,* 3195–3198, 1995.

Lockwood, M., and R. Stamper, Long-term drift of the coronal source magnetic flux and the total solar irradiance, *Geophys. Res. Lett., 26,* 2461–2464, 1999.

Schatten, K. H., J. M. Wilcox, and N. F. Ness, A model of interplanetary and coronal magnetic fields, *Sol. Phys., 6,* 442–455, 1969.

Slavin, J. A., G. Jungman, and E. J. Smith, The interplanetary magnetic field during solar cycle 21: ISEE-3/ICE observations, *Geophys. Res. Lett., 13,* 513–516, 1986.

Wang, Y.-M., S. H. Hawley, and N. R. Sheeley, Jr., The magnetic nature of coronal holes, *Science, 271,* 464–469, 1996.

Wang, Y.-M., A. G. Nash, and N. R. Sheeley, Jr., Evolution of the Sun's polar fields during sunspot cycle 21: Poleward surges and long-term behavior, *Astrophys. J., 347,* 529–539, 1989.

Wang, Y.-M., and N. R. Sheeley, Jr., On potential field models of the solar corona, *Astrophys. J., 392,* 310-319, 1992.

Wang, Y.-M., and N. R. Sheeley, Jr., Solar implications of Ulysses interplanetary field measurements, *Astrophys. J., 447,* L143–L146, 1995.

J. Lean, N. R. Sheeley, Jr., and Y.-M. Wang, E. O. Hulburt Center for Space Research, Naval Research Laboratory, Washington, DC 20375-5352. (e-mail: lean@demeter.nrl.navy.mil; sheeley@spruce.nrl.navy.mil; ywang@yucca.nrl.navy.mil)

(Received September 29, 1999; revised November 13, 1999; accepted November 22, 1999.)